Starvation Modeling and Identification in Dense 802.11 Wireless Community Networks

Cunqing Hua and Rong Zheng

Department of Computer Science
University of Houston
Houston, TX, 77204, USA
http://www.cs.uh.edu

Technical Report Number UH-CS-07-10

August 13, 2007

Keywords: 802.11 wireless community networks, starvation, modeling, carrier sense, hidden node

Abstract

With the growing number of spontaneously deployed WiFi hotspots and home networks, end-users often experience significant performance degradation or even starvation. However, we observe that tuning individual system parameter (channel, Tx power, carrier sense (CS) threshold, and transmit rate etc.) is insufficient and in some cases may lead to starvation. In this paper, we develop a comprehensive analytical model to characterize throughput of individual flows in dense 802.11 wireless community networks. The proposed model subsumes existing models for 802.11 MAC in multihop wireless networks by accounting for heterogeneous transmission power levels and CS thresholds, as well as various sources of packet collisions. Based on the insight from the theoretical analysis and simulation results, we propose a simple identification mechanism that determines the sources of starvation using local measurements. Both the theoretical model and identification algorithm are validated using ns-2 simulations.

Starvation Modeling and Identification in Dense 802.11 Wireless Community Networks

Cunqing Hua and Rong Zheng

Abstract

With the growing number of spontaneously deployed WiFi hotspots and home networks, end-users often experience significant performance degradation or even starvation. However, we observe that tuning individual system parameter (channel, Tx power, carrier sense (CS) threshold, and transmit rate etc.) is insufficient and in some cases may lead to starvation. In this paper, we develop a comprehensive analytical model to characterize throughput of individual flows in dense 802.11 wireless community networks. The proposed model subsumes existing models for 802.11 MAC in multihop wireless networks by accounting for heterogeneous transmission power levels and CS thresholds, as well as various sources of packet collisions. Based on the insight from the theoretical analysis and simulation results, we propose a simple identification mechanism that determines the sources of starvation using local measurements. Both the theoretical model and identification algorithm are validated using ns-2 simulations.

Index Terms

802.11 wireless community networks, starvation, modeling, carrier sense, hidden node

I. Introduction

In recent years, there has been a rapid growth in the deployment of wireless LANs in a wide variety of settings, such as residential areas, shopping malls, airports, office and campus buildings. In contrast to managed networks found in office and campus buildings, which are carefully planned with optimized base station placement, channel assignments, power control, association and access control [3], [15], home networks and community networks are generally poorly configured and managed. Spontaneous deployment of dense 802.11 wireless LANs can cause substantial performance degradation to end-users. For instance, Akella *et al.* [2] observed that most 802.11 users employ default, factory-set configurations for key parameters such as the transmission channel, which can lead to serious channel contention in dense deployments. Several recent work advocates the need for distributed coordination among wireless devices by tuning individual system parameters, i.e., through power control [2], rate adaptation [10], [22], channel-hopping [18], channel assignment [16], [17], and carrier sense (CS) threshold adaptation [20]. However, two challenges remain to be addressed:

- Characterization of the compound effects and stability of adjusting multiple system parameters. For example, what is the proper time scale to adjust power and transmission rate for time-varying fading channels? When and how often should carrier sensing threshold be changed?
- Design of localized algorithms using local measurements in improving per-node and system-wide performance. Localized solutions are desirable in allowing incremental upgrade of WLAN access points (APs) and client devices.

As an initial step to address these problems, in this paper, we focus on flow starvation scenarios due to poorly configured system parameters (or possibly as a result of distributed coordination mechanisms). In addition to well-known sources of starvation such as *carrier sense starvation* and *hidden node starvation*, we identify a third cause of starvation, i.e., *asymmetric sense starvation*, which is likely to be prevalent in dense wireless community networks with heterogeneous transmission power levels and asymmetric channel conditions.

To characterize the effect of asymmetric sense, we develop a comprehensive theoretical model to analyze the throughput of link-level flows in 802.11 wireless community networks. Our model subsumes existing analytical models for multihop 802.11 networks, which assume a *common* Tx power level, CS threshold and transmit data rate among all nodes [7], [8], [21]; and thus may be of independent interest in its own right. The key of our analysis is to model the evolution of channel states observed by a "typical" node as a renewal process. Using second-order approximation techniques similar to those adopted in [7], the throughput of individual nodes is determined by solving a set of fixed-point equations via numerical methods. In deriving packet loss probability experienced by

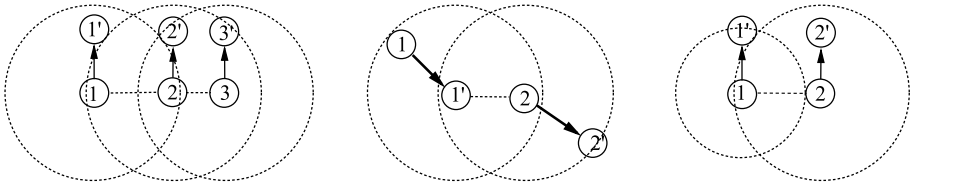

(a) carrier sense starvation (b) hidden node starvation (c) asymmetric sense starvation

Fig. 1: Flow throughput starvation examples. (Circular disks give the CS range; dashed lines indicate the carrier sense relations of two nodes, and the solid directed lines give the link flows with arrows pointing from transmitter to receiver.)

individual flows, we take into account collisions caused by nodes within carrier sensing range, hidden nodes as well as asymmetric sense.

Our proposed model and simulation study reveal that an effective starvation mitigation solution requires judicious adjustment of different system parameters based on the dominating cause of starvation. To accomplish this, we propose a simple identification mechanism that can determine the sources of starvation using solely local measurements. Effectiveness of the proposed algorithm is validated through packet-level simulations in ns-2 [1].

Main Contributions: In the paper, we make the following contributions:

- A classification of sources of flow starvation in dense 802.11 wireless community networks.
- A comprehensive model for performance analysis in multihop 802.11 wireless networks with heterogeneous Tx power levels and CS thresholds.
- A simple starvation identification mechanism that determines sources of starvation via local measurement.

The rest of the paper is organized as follows. In Section II, we discuss three sources of starvation and summarize existing solutions. The physical layer models and notations are introduced in Section III. In Section IV, we derive the throughput of individual link flow using the renewal theory. The analytical results are validated in Section V. A starvation identification algorithm is proposed and evaluated in Section VI, and finally we conclude the paper in Section VII.

II. Motivation and Related Work

Nodes in dense wireless community networks may suffer from intensive contention from neighboring transmitters. As a result, some flows may be starved and refrained from transmissions for a prolonged period of time. MAC layer starvation has serious implication to the performance observed by end-users when interacting with TCP-like congestion control protocols or QoS-sensitive streaming applications. We have identified three types of starvation:

- **Carrier sense (CS) starvation** results in low transmission opportunities due to the innate unfairness of the IEEE 802.11 DCF protocol. As shown in Fig. 1(a), there are three parallel flows where node 2 can sense both node 1 and 3. Node 1 and 3 cannot sense each other. The transmissions of nodes 1 and 3 can overlap for a prolonged time. As a result, node 2 almost always finds a busy channel and freezes its back-off counter.
- **Hidden node starvation** arises when there are concurrent transmitters outside the carrier sensing range of a transmitter node but within the interference range of its receiver node. In Fig. 1(b), node 2 cannot sense the transmissions of node 1, but it can interfere with its receiver node $1'$. As a result, packets sent by node 1 will be lost at node $1'$, and flow 1–$1'$ is starved. It should be noted that if node 1 and 2 are hidden nodes with respect to each other, then both flows can still contend the channel fairly and no single one is starved.
- **Asymmetric sense starvation** is caused by heterogeneous transmission power levels, CS thresholds or asymmetric channel conditions among pairs of transmitter nodes. In Fig. 1(c), node 1 cannot sense node 2, but node 2 can sense node 1. As a result, transmissions from node 1 can collide with node 1's ongoing transmissions due to hidden node. Furthermore, node 1 always finds the channel to be idle and can access the channel whenever it has packet to send, while node 2 has to freeze its back-off counter when it detects node 1's transmissions. Therefore, asymmetric sense starvation is a combination of hidden node and carrier sense starvation.

Note that we cannot distinguish between asymmetric sense and a combination of hidden node and carrier sense starvation caused by different nodes without detailed packet traces.

Existing work: Several studies show that the flow starvation can be mitigated by tuning the system parameters individually (e.g., channel, Tx power, CS threshold, and Tx data rate etc.) of the wireless devices. For example, in [8], Garetto *et al.* investigate the starvation problem in multihop wireless networks and propose a centralized rate-limiting policy. In [14], Mhatre *et al.* investigate the problem of tuning the transmit power to mitigate interference in high density 802.11 WLANs. In [19], a multi-channel coordination protocol is proposed to address the starvation problem.

The idea of tuning the transmit power and CSMA parameters has been explored for improving the network performance for both wireless LANs and multihop networks. In [2], Akella *et al.* propose power control and rate selection algorithms and their results shown significant benefits can be gained from these algorithms. In [20], Vasan *et al.* propose the ECHOS algorithm that aims to improve the capacity of 802.11 hotspots by dynamically adjusting the CS threshold. In [23], Yang and Vaidya study the impact of physical carrier sense on spatial reuse in multihop wireless networks. In [11], Kim *et al.* show that network capacity depends only on the ratio of Tx power and CS threshold, and propose an algorithm to adjust the Tx power and data rate based on perceived SINR at the sender side. Zhai and Yang [24] propose a spatial reuse optimization solution for multihop, multi-rate wireless networks. They consider variable transmission distances, different receiver sensitivities and multihop forwarding effects. Lin and Hou [12] consider the MAC layer behavior of IEEE 802.11 DCF and derive the network capacity based on Cali's model [5].

III. Models and Notations

We consider a dense 802.11 wireless community network with many APs and client stations distributed in close proximity. The network is operated in *infrastructure mode*. Thus, all transmissions are either initiated from client stations to the associated AP (*uplink* transmissions), or from APs to the client stations (*downlink* transmissions). We assume that the basic mode of IEEE 802.11 distributed coordinated function (DCF) protocol is used. In this mode, a node needs to detect the channel before it can transmit a packet, which is known as *physical carrier sense*. If the channel is free for a specific time, it can continue the transmission, otherwise it has to defer the transmission and enter a back-off procedure. After the back-off procedure is finished, the same carrier sense process is repeated until it sends out the packet. We do not model the exchange of RTS/CTS messages before packet transmissions, however, our analysis can be easily extended to this case.

Let P_{tx} and P_{rx} denote the Tx power at a sender and the received signal strength at the receiver respectively. Their relation can be characterized by the path-loss radio propagation model as $P_{rx} = \frac{GP_{tx}}{r^{\theta}}$, where G is the constant antenna gain, r is the distance between the sender and the receiver, and θ is the path loss exponent that typically ranges from 2 to 4.

According to 802.11 DCF protocol, if the sensed signal level is above the CS threshold T_{cs}, the medium is assumed to be busy and the node should defer its transmission. Let $\mathcal{C}(i)$ denote the set of nodes that node i will sense the medium to be busy if any one of these nodes is transmitting. We have

$$\mathcal{C}(i) = \left\{ j \left| \frac{P_{tx}(j)}{r(i,j)^{\theta}} \geq T_{cs}(i), \forall j \right. \right\} \tag{1}$$

Suppose all nodes adopt the same Tx power and CS threshold, if a node i can sense the transmission of node j, then node j also can sense node i if it is transmitting, we referred this as *symmetric sense*. The set of *symmetric sense* nodes of a node is a subset of its carrier sense nodes as

$$\mathcal{SC}(i) = \{ j \,|i \in C(j), \forall j \in C(i) \}\, multiple \tag{2}$$

On the other hand, if heterogeneous Tx power or CS threshold are adopted by different nodes due to power control or CS adaptation algorithms, a node pair may have *asymmetric sense* that only one of them can hear from the other. We define the set of *asymmetric sense* nodes as a subset of its carrier sense nodes as

$$\mathcal{AC}(i) = \{ j \,|i \notin C(j), \forall j \in C(i) \} \tag{3}$$

A policy that requires $\mathcal{AC}(i) = \emptyset \ \forall i$ is termed *symmetric sense policy*.

Let $\mathcal{H}(i)$ denote the set of hidden nodes who cannot sense the transmission of node i, but they can interfere the receiver node i'. Thus, if the transmission from hidden nodes overlaps with the transmission of node i, it will lead to collision at the receiver i'. That is

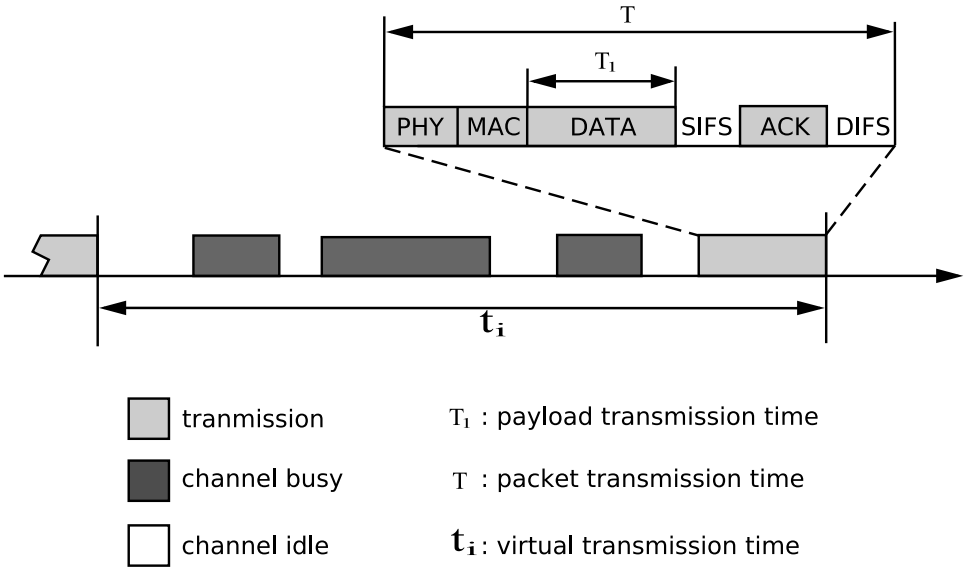

Fig. 2: Virtual transmission time and packet transmission time

$$\mathcal{H}(i) = \left\{ j \left| \frac{P_{tx}(i)/r^{\theta}}{P_{tx}(j)/r(i',j)^{\theta}} < \beta, j \notin \mathcal{C}(i) \right. \right\} \tag{4}$$

where β is the required signal to interference ration (SIR) threshold such that the receiver i' can correctly decode the packet.

Nodes within carrier sensing range may be synchronized in transmission attempts at the same time slot boundaries. We denote the set of *coordinated nodes* $\mathcal{CO}(i)$ of node i as the nodes that both sender i and receiver i' are in their transmission ranges. That is

$$\mathcal{CO}(i) = \left\{ j \left| j \in C(i), j \in C(i'), \forall j \right. \right\} \tag{5}$$

IV. Throughput Analysis

Several models have been developed to analyze link level throughput in multihop wireless networks in the literature [7], [8]. However, all the models assume a common Tx power level and CS threshold at all nodes. Furthermore, they often ignore collisions among nodes within carrier sensing range and treat their transmissions as non-overlapping. Both assumptions are not valid in dense community networks. Our model also differs from [7] in that our goal is to compute the throughput of each node in the network, which is not known a prior and has to be computed iteratively by solving a set of fixed point equations.

From the perspective of an individual node, i, the channel can be in three different states: (i) *self-channel* when the channel is occupied by the transmission of node i itself; (ii) *busy-channel* when the channel is occupied by the transmissions of other nodes; (iii) *idle-channel* when the channel is not used by any node. Let x_i, y_i and z_i denote the probabilities that the channel is seen in these three states by node i, then the throughput S_i of node i is given by

$$S_i = x_i \times (1 - p_i) \times R_i \times \frac{T_1}{T} \tag{6}$$

where p_i is the conditional loss probability, R_i is the data transmission rate, T_1 is the transmission time of the data payload, and $T = T_H + T_1 + DIFS + SIFS + ACK$ is the overall transmission time for a packet including PHY and MAC header, data payload and ACK, as well as DIFS and SIFS. We assume that R_i is fixed for each node, and T_1 and T are known a prior, so it is sufficient to obtain the throughput by deriving the transmission probability x_i and loss probability p_i. In this section, we first derive the transmission probability and loss probability, then discuss the procedure that iteratively computes these two quantities and obtain the throughput using (6).

A. Transmission Probability

We assume that the channel state observed by a node i can be described by a renewal process, where a renewal period is defined as the time interval between two consecutive transmissions from node i as shown in Fig. 2, which is also referred to as the virtual transmission time, and t_i is the average length of the renewal period.

Each renewal period consists of idle periods, multiple busy periods due to the transmissions of other nodes, and ends with the transmission by node i. Let X_i, Y_i, Z_i denote, respectively, the *self-channel*, *busy-channel* and *idle-channel* times in a renewal period. Clearly, $t_i = |X_i| + |Y_i| + |Z_i|$. Since there is only one transmission from node i in each renewal period, we have $|X_i| = T$. For idle period, as seen from Fig 2, node i will defer the backoff procedure as soon as the channel is busy, and resume the process when the channel is free. We assume that nodes attempt to transmit in an idle slot following independent Bernoulli distribution with probability τ_i. Therefore, $|Z_i| = 1/\tau_i$, where τ_i is the attempt probability in an idle slot, which is a function of packet loss probability p_i as derived in [4].

$$\tau_i = \frac{2(1-2p_i)}{(1-2p_i)(W_0+1) + p_i W_0(1-(2p_i)^N)} \tag{7}$$

where W_0 is the minimum contention window size and N is the maximum number of backoff stages, that is, the maximum contention window size is equal to $2^N W_0$.

Using the regenerative property of the renewal process, the transmission probability, busy probability and idle probability are given by

$$\begin{aligned} x_i &= \frac{|X_i|}{t_i} = \frac{T}{|X_i| + |Y_i| + |Z_i|} \\ y_i &= \frac{|Y_i|}{t_i} = \frac{|Y_i|}{|X_i| + |Y_i| + |Z_i|} \\ z_i &= \frac{|Z_i|}{t_i} = \frac{1/\tau_i}{|X_i| + |Y_i| + |Z_i|} \end{aligned}$$

Therefore, the transmission probability x_i can be expressed as a function of the idle probability z_i as

$$x_i = z_i \times \tau_i \times T \tag{8}$$

Since $z_i = 1 - x_i - y_i$, from (8) we have

$$x_i = (1 - x_i - y_i) \times \tau_i \times T \tag{9}$$

To find x_i from Eq. (9), we need to derive the busy probability y_i. Note that the *busy-channel* time Y_i seen by node i is the union of the transmission times of node i's neighboring nodes, that is,

$$|Y_i| = |\bigcup_{j \in \mathcal{AC}(i)} X_j| \approx \sum_{j \in \mathcal{AC}(i)} |X_j| - \sum_{m,n \in \mathcal{AC}(i)} |X_m \bigcap X_n| \tag{10}$$

where the union of the transmission time is decomposed using the inclusion-exclusion principle and approximated by the second-order intersection of transmission times.

The intersection of the transmission time of any two nodes m and n depends on their topological relations. In the following, we derive this value by considering two scenarios: (i) nodes m and n have no common neighbors, (ii) nodes m and n cannot hear each other, but they have common neighbors.

If nodes m and n have no common neighbors, there are three possible cases as shown in Fig. 3:

(1) Nodes m and n cannot sense each other, that is, $m \notin C(n)$ and $n \notin C(m)$, we assume their transmission times can overlap arbitrarily. Consider a specific transmission from node m with duration T, since node n can start transmission at any point during this interval, the expected overlapping length of their transmission time is $(1-(1-z_n\tau_n)^T) * T/2$, where $z_n\tau_n$ is the attempt probability per time slot. Similarly, if node n starts transmission first, the expected overlapping length during a transmission is $(1-(1-z_m\tau_n)^T) * T/2$. Since the number of transmissions from node m and n in a renewal period are $t_i x_m/T$ and $t_i x_n/T$ respectively, we can obtain the intersection of transmission time of nodes m and n as

$$\begin{aligned} |X_m \bigcap X_n| &= t_i x_m (1-(1-z_n\tau_n)^T)/2 \\ &+ t_i x_n (1-(1-z_m\tau_m)^T)/2 \end{aligned} \tag{11}$$

(2) Nodes m and n have *symmetric sense*, that is, $m \in C(n)$ and $n \in C(m)$, so they can sense the transmission of each other. We consider two scenarios: (i) nodes m and n are coordinated nodes, so their transmissions may overlap if they attempt to transmit at the same time slot. Without loss of generality, suppose that node n attempts at the same time as node m, then the expected overlapping length is $z_n\tau_n T$, which is equal to x_n. Given that on average there are $t_i x_m/T$ transmissions from node m, the overall intersection of their transmission

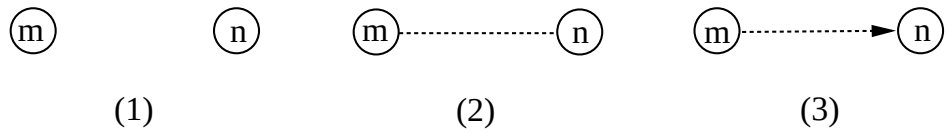

Fig. 3: Carrier sense of two nodes without common neighbor

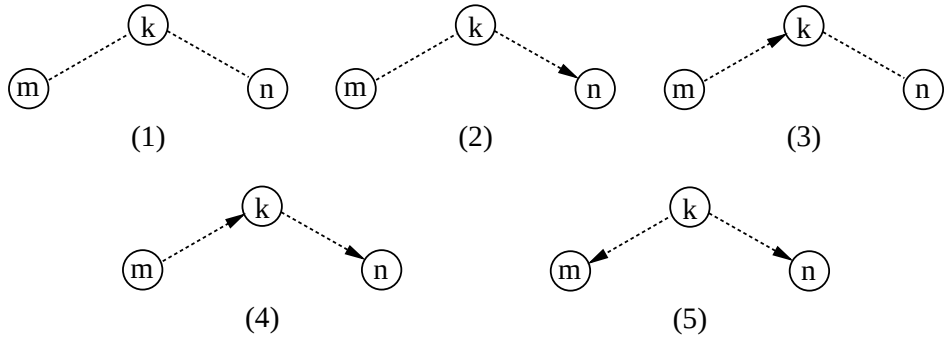

Fig. 4: Carrier sense of two nodes with common neighbor

times is given by $t_i x_m x_n / T$. (ii) node m and n are not coordinated nodes, we assume that their transmissions are not synchronized, the intersection of their transmission time is zero. In summary, the intersection of the transmission times in these two cases is

$$|X_m \bigcap X_n| = \begin{cases} t_i x_m x_n / T, & \text{if } m \in \mathcal{CO}(n) \\ & \text{and } n \in \mathcal{CO}(m) \\ 0, & \text{otherwise.} \end{cases} \tag{12}$$

(3) Nodes m and n have *asymmetric sense*. Without loss of generality, we assume $m \in AS(n)$ and $n \notin AS(m)$ as shown in Fig 3(c). In this case, their transmission times can overlap only if node n transmits first, and node m starts transmission during this interval since it cannot sense the transmission of node n. Following the derivation of first case, we have

$$|X_m \bigcap X_n| = t_i x_n (1 - (1 - z_m \tau_m)^T)/2 \tag{13}$$

If node m and n cannot sense each other, but they have a common neighbor k. Their relations with node k can be either symmetric sense or asymmetric sense, therefore there are five possible scenarios as shown in Fig. 4:

(1) Both node m and n have *symmetric* sense with node k, we assume that they cannot transmit during the transmission time of node k, so the "sample space" within which m and n may overlap is $t_i - |X_k|$.

(2) Node m and k have symmetric sense, but n has asymmetric sense with node k (i.e, $k \in AS(n)$), then the amount of time that transmissions from node n may overlap with node m is given by $(|X_n| - |X_k \bigcap X_n|)$, and the "sample space" within which m and n may overlap is $t_i - |X_k|$.

(3) Node m and k have asymmetric sense, but n and k has symmetric sense (i.e.,$m \in AS(k)$ and $k \in SC(n)$). Similar to the previous scenario, the amount of time that transmissions from node m may overlap with node m is $(|X_m| - |X_m \bigcap X_k|)$, and the "sample space" within which m and n may overlap is $t_i - |X_k|$.

(4) Both m and n have asymmetric sense with k (i.e., $m \in AS(k), k \in AS(n)$), then the amount of transmission time of node m that may overlap with that of node n is $(|X_m| - |X_m \bigcap X_k|)$, and the amount of transmission time of node n that may overlap with that of node m is $(|X_n| - |X_k \bigcap X_n|)$. The "sample space" within which m and n may overlap is $t_i - |X_k|$.

(5) Both m and n have asymmetric sensing with k($k \in AS(m), k \in AS(n)$), similar to previous cases, the amounts of transmission time of node m and node n that may overlap with each other are $(|X_m| - |X_k \bigcap X_m|)$ and $(|X_n| - |X_k \bigcap X_n|)$ respectively, and the "sample space" within which m and n may overlap is $t_i - |X_k|$.

In summary, the intersection of the transmission times of nodes m and n in these five scenarios can be expressed as

$$|X_m \bigcap X_n| = \frac{1}{t_v - |X_k|}\Big[(|X_m| - |X_m \bigcap X_k|)(1-(1-z_n\tau_n)^T)/2 + (|X_n| - |X_n \bigcap X_k|)(1-(1-z_m\tau_m)^T)/2\Big] \tag{14}$$

B. Packet Loss Probability

The transmission of node i can fail due to the concurrent transmissions from neighboring nodes. We identify three events that will lead to packet loss: (i) collision between coordinated nodes; (ii) collision due to hidden nodes, and (iii) collision due to asymmetric sense. Let p_{ik} denote the loss probability due to the collision by node k, then the overall packet loss probability on link (i, i') can be expressed as

$$p(i) = 1 - \prod_{k \in \mathcal{CO}(i)} (1 - p_{ik}) \prod_{k \in \mathcal{H}(i)} (1 - p_{ik}) \prod_{k \in \mathcal{AS}(i)} (1 - p_{ik}) \tag{15}$$

Coordinated Node Collision: Suppose that node k is a coordinated node of node i, then the collision between them occurs if and only if node k detects the channel to be free and attempts to transmit at the same time slot as node i. Therefore, the probability of collision caused by node k is equal to its attempt probability in an idle slot, that is, $p_{ik} = \tau_k$.

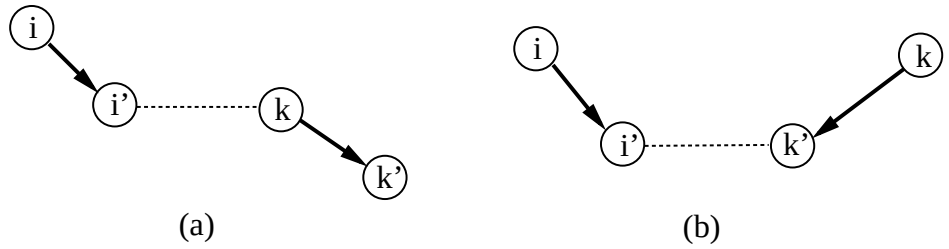

Fig. 5: Hidden node collision scenarios

Hidden Node Collision: We consider two hidden node scenarios as shown in Fig. 5:

(a) Node k is a hidden node of node i, and node i' is within the interfering range of node k as shown in Fig. 5(a). In this case, the collision will occur at node i' if node k starts its transmission before node i and their transmissions overlap with each other, or it starts its transmission during the transmission of node i. Therefore, the maximum possible overlapping length is twice of the payload transmission time, or $2T_1$. Consequently, the collision probability is the probability that node k makes an attempts in this interval, that is

$$p_{ik} = 1 - (1 - z_k\tau_k)^{2T_1} \tag{16}$$

(b) Node k is a hidden node of link (i, i'), and the receiver i' is outside the interfering range of node k but within that of node k' as shown in Fig. 5(b). In this case, the collision will occur at node i' if node k starts its transmission before node i, and the ACK sent by node k' collides with the data at node i'. However, since data transmission from node k is subject to collisions caused by other nodes, node k' will not send an ACK if it fails to receive the packet. As a result, the effective probability of node k' sending ACK is only $z_k\tau_k(1-p(k))$. Since the possible overlapping length of their transmission times is T_1, the collision probability is given by

$$p_{ik} = 1 - [1 - z_k\tau_k(1 - p(k))]^{T_1} \tag{17}$$

Asymmetric Sense Collision: There are two possible scenarios where asymmetric sense may lead to collision as shown in Fig. 6:

(a) Nodes i and k have asymmetric sense as shown in Fig.6(a), and node k cannot hear the transmission from i. In this case, node k may start its transmission during the transmission of node i, which will lead to collision at node i when the ACK is sent back from node i'. The possible overlapping time is T_1. We then have

$$p_{ik} = 1 - (1 - z_k\tau_k)^{T_1} \tag{18}$$

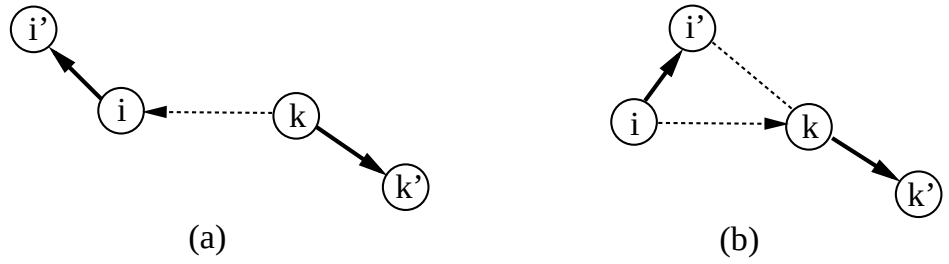

Fig. 6: Asymmetric sense collision scenarios

(b) Nodes i and k have asymmetric sense as shown in Fig.6(b), and node i cannot sense the transmission from k, but its receiver i' is within the interfering range of node k. In this case, node i may start transmission during the transmission of node k, since receiver i' is interfered by the transmission from node k, collision will occur. The possible overlapping time duration is also T_1, so the collision probability is

$$p_{ik} = 1 - (1 - z_k \tau_k)^{T_1} \tag{19}$$

C. Throughput Computation

With the transmission probabilities x_i's, by substituting them in (10) and (15), we can obtain the busy probabilities y_is and packet loss probabilities p_is, from which we can derive the attempt probabilities τ_i's using (7). Plugging y_is and τ_is in (9), we can obtain new set of transmit probabilities x_is. This process can be repeated iteratively as that used in [4] and [7] for single-cell and multihop 802.11 networks. Finally, we can obtain the transmission probabilities x_is and loss probabilities p_is, and compute the through of all flows using (6).

V. Simulation and Model Validation

In this section, we validate the analytical model using ns-2 simulation. All the flows in the simulation are assumed to be saturated sending UDP packet at the maximum data rate (i.e., 11Mbps). The parameters used in the simulations are listed in Table I. Some insights are also drawn on the effect of adjusting individual system parameters. To quantify the starvation problem in these three settings, we adopt the fairness index as introduced in [9], i.e., $F = \frac{(\sum S_i)^2}{n \sum S_i^2}$, where S_i is the throughput of ith flow. F is a value between 0 and 1, and the maximum value of 1 is achieved if all n flows receive equal throughput.

TABLE I: Parameters Setting for Simulation

Parameter	Value
Propagation model	TwoRayGround
Packet size	1500 bytes
ACK size	44 bytes
UDP header	20 bytes
MAC header	28 bytes
PHY header	24 bytes
BasicRate	1 Mbps
DataRate	11 Mbps
Slot time	20 us
SIFS/DIFS/EIFS	10/50/363 us
(CW_{min}, CW_{max})	(31, 1023)
Retry limit	7

A. Random topology

In this section, we compare the analytical and simulation results on a random network with 15 links randomly distributed over a $1000m \times 1000m$ square, and the link distances are drawn randomly in [0, 100] meter. We consider three different settings for Tx power and CS threshold to represent for typical power control schemes:

- *Common Tx Power and CS threshold*: transmission range and CS range are set equal to 200m and 400m respectively for all nodes.

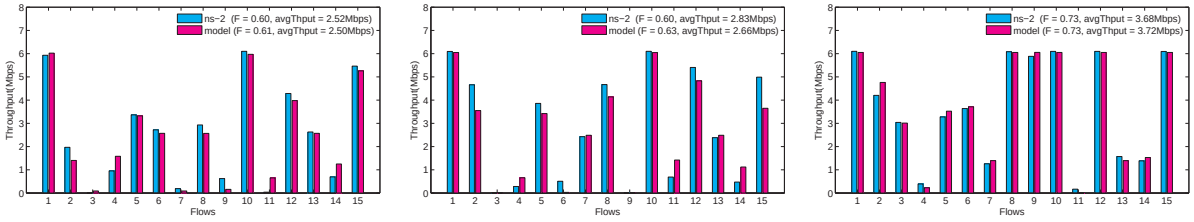

(a) Common Tx power (b) Heterogeneous Tx power (c) Symmetric Tx power

Fig. 7: Flow throughput in a random network

- *Heterogeneous Tx Power and CS threshold*: transmission range are set equal to the link distance, and CS range is set equal to twice of the link distance.
- *Symmetric Tx Power and CS threshold*: transmission range are set equal to the link distance, and CS threshold is set to a value such that the product of Tx power and CS threshold is kept constant and equal to that in the common power case. It is proved in [14] that this condition suffices to remove asymmetric links in the network under symmetric channel models.

Fig. 7 compares the analytical and simulation results under the three settings in the random network. From Fig. 7, we can see that the analytical results generally match well with the simulation results, and the fairness index computed by our model is very close to that obtained from the simulation. As shown in Fig. 7(a), for the common Tx power setting, five flows are close to starvation due to channel contention and hidden node problems. The starvation problem is partially alleviated by adjusting the Tx power proportional to the link distance as shown in Fig. 7(b). However, some flows still experience low throughput since the Tx power and CS threshold setting in this case is insufficient to remove the hidden node problem. Furthermore, heterogeneous Tx power also leads to asymmetric sense collisions to some nodes. In the third setting, by adjusting the Tx power while maintaining the product with the CS threshold of all nodes, asymmetric links can be avoided in the network. The starvation problem is alleviated compared with previous two settings as shown in Fig. 7(c). However, this solution cannot entirely solve the starvation problem as demonstrated in the low throughput of flow 4 and 11. From the perspective of the fairness index, we can see that the first setting is the worst where the fairness index is around 0.6, and the third setting can improve the fairness index to around 0.7.

B. Grid Topology

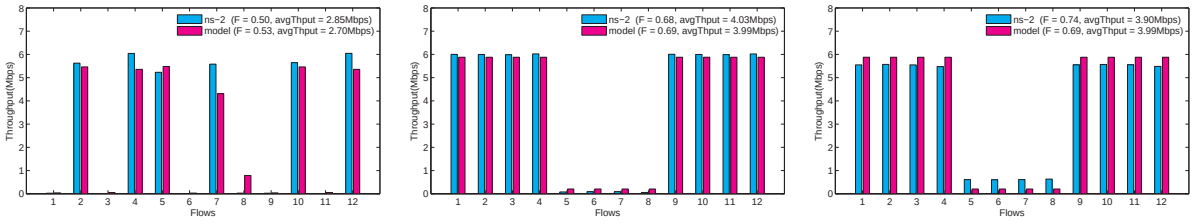

(a) Common Tx power (b) Heterogeneous Tx power (c) Symmetric Tx power

Fig. 8: Flow throughput in a grid network

We also design a grid topology as shown in Fig. 9, where every transmitter node is a hidden node to its left neighbor flow, while the outer flows on each column may cause CS starvation to the middle flow on the same column. Fig. 8 compares the analytical and simulation results under the three settings in the grid network. With common transmission power, flow 8 suffers from carrier sense starvation; flow 1, 3, 9 and 11 suffer from hidden node starvation; and flow 6 experiences both types of starvation caused by flow 7, flow 10 and 2. The last case

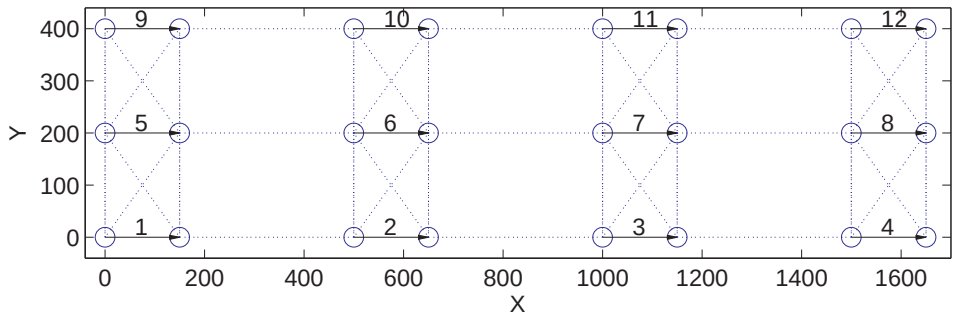

Fig. 9: Grid network topology

is similar to asymmetric starvation with the differences that hidden node and carrier sense starvation are induced by different flows. The results for heterogeneous Tx power and symmetric Tx power schemes are similar. In both cases, all transmitters use a common but minimum power to reach the respective receiver nodes. This effectively eliminates the hidden node problem as a transmission would not cause interference to its left-hand neighbor flow. However, carrier sensing starvation still exists as evident from Fig. 8(b)-(c), where flow 5 – 8 are all starved. Again, the theoretical model we develop gives very consistent results in both throughput achieved by individual flows as well as fairness indices.

VI. Starvation Identification

The proposed model and simulation study in the previous section reveal that an effective starvation mitigation solution involves judicious adjustment of different system parameters based on the dominating source of starvation. In dense wireless community networks, it is often difficult or infeasible to obtain information regarding the set of contending stations and their respective throughput and loss probability. A key challenge is thus how to infer the possible causes of starvation using *local* information in a robust manner. This is particularly difficult as a node cannot determine which nodes collide with it in event of packet losses. In [6], [13], MAC-layer behaviors are analyzed by deploying distributed sniffer nodes. Detailed packet level traces can be obtained and combined if the sniffer nodes are well synchronized. We do not assume availability of densely placed sniffers, nor additional communication between nodes.

Consider a link flow that suffers from a low throughput. Under the normal protocol behavior, it can be attributed to several reasons (or a combination of them), namely, i) existence of hidden nodes, ii) existence of multiple "mice" flows on coordinated nodes (i.e., in a single hop network) and iii) existence of a small number of "elephant" flows (as in the case of the carrier sensing starvation). The objective of the starvation identification algorithm is to identify the dominating cause among the three.

The design of the proposed starvation identification algorithm is motivated by the following observations:

- In *carrier sense starvation*, a flow has little transmission opportunity but can still have high packet delivery ratio once it obtains the channel.
- In *hidden node starvation*, a flow may suffer from high packet loss in each attempt.
- When a node contends with a large number of coordinated nodes in a fair manner, the number of contention station can be determined from the measured loss probability and throughput.
- In *asymmetric sense starvation*, the primary cause of starvation is hidden node starvation, which leads to high loss probability and the secondary is the carrier sensing starvation, which results in low transmission opportunities.

Let p_i and S_i be the observed loss probability and throughput of node i. We define a *hypothetical collision probability* p_i^H of node i as the collision probability when a node gets a fair share of the channel when contending with $n-1$ coordinated nodes. Under this hypothesis, the transmission probability of node i is given by:

$$x_i = (1 - x_i - y_i)\tau_i T \approx [1 - x_i - (n-1)x_i]\tau_i T \tag{20}$$

The second equality is obtained by approximating the busy probability y_i with the sum of transmission probabilities from other contending nodes assuming all nodes have the same transmission probability. Solving this equation for n, and substituting x_i with S_i from Eq. (6), we have

$$n \approx \frac{1}{x_i} - \frac{1}{\tau_i T} = \frac{R(1-p_i)}{S_i}\frac{T_1}{T} - \frac{1}{\tau_i T} \tag{21}$$

Consequently, the hypothetical collision probability is $p_i^H = 1-(1-\tau_i)^{n-1}$, where τ_i is a function of p_i given by Eq. (7). By comparing the hypothetical collision probability with the measured loss probability, we can distinguish starvation due to carrier sensing and hidden nodes.

The asymmetric sense starvation cannot be distinguished from hidden node starvation based on packet loss probabilities since both can potentially lead to high packet losses. However, we observe that nodes can sense the transmission of its asymmetric sense neighbors, but cannot sense the transmissions of hidden nodes. As a result, the perceived busy time should be higher if the node has an asymmetric sense neighbor other than a hidden node. Suppose that node i has a hidden/asymmetric sense node k. Define the *hypothetical Tx probability* x_k^H to be the Tx probability of node k. Combining Eq. (18) and $x_k = z_k \tau_k T$, we have

$$x_k^H = T \times (1-(1-p_i)^{1/T_1}) \tag{22}$$

The busy probability y_i of node i, can be derived from its throughput S_i and loss probability p_i using Eq. (6) and (8) as

$$y_i \quad = \quad 1 - \frac{S \times T}{(1-p_i) \times R_i \times T_1}(1 + 1/\tau_i T) \tag{23}$$

Finally, by comparing the hypothetical Tx probability x_k^H with y_i, we can distinguish starvation due to asymmetric sense from hidden nodes.

Toward this end, we propose a simple identification mechanism in Algorithm 1, where α and β are two system parameters.

Algorithm 1 Starvation identification algorithm

```
Given a starved flow i,
if p_i^H ≤ p_i × α or p_i ≥ 0.5 then
    Hidden node starvation detected;
    if x_k^H ≤ y_i/β then
        Asymmetric sense starvation detected;
    end if
else if p_i^H ≥ p_i/α then
    Carrier sensing starvation detected;
else
    Contention due to coordinated nodes;
end if
```

To validate this scheme, we have conducted extensive simulations in ns-2. Due to space limit, only a subset of results are presented. In all experiments, each flow has infinitely backlogged packets. The loss probability and throughput of each flow are measured from the simulation; and other quantities are derived from the above equations.

Grid topology: We examine the grid network discussed in Section V-B for the common Tx power case. Recall that in the grid network, flow 8 suffers from carrier sense starvation; flow 1, 3, 9 and 11 suffer from hidden node starvation; and flow 6 experiences both types of starvation. Fig. 10 gives loss probability and hypothetical collision probability for all link flows. From the top graph, we can see that the hypothetical loss probability of flow 8 is much higher than its loss probability, so it is identified as carrier sense starvation. Flows 1, 3, 9 and 11 experiences higher loss probabilities than hypothetical collision probability; flow 6 has a loss probability greater than 0.5. Therefore, they are identified as hidden node starvation. In addition, from the bottom graph, flow 6 has higher busy probability compared with x^H, therefore it is further classified as suffering from both hidden node and carrier sensing starvation.

Random topology: In this set of experiments, we conduct simulation runs of 50 randomly generated networks consisting of 15 node pairs. A transmitter sets the minimal transmission power needed reach its receiver node. The measured and inferred metrics of starved flows (with less than 0.5Mbps throughput) are plotted in Fig. 11 and Fig. 12. We manually check the topologies to determine the ground truth. For comparison, also depicted in Fig. 11 are results from a single hop network consisting of only coordinated nodes with links ranging from 5 to 15.

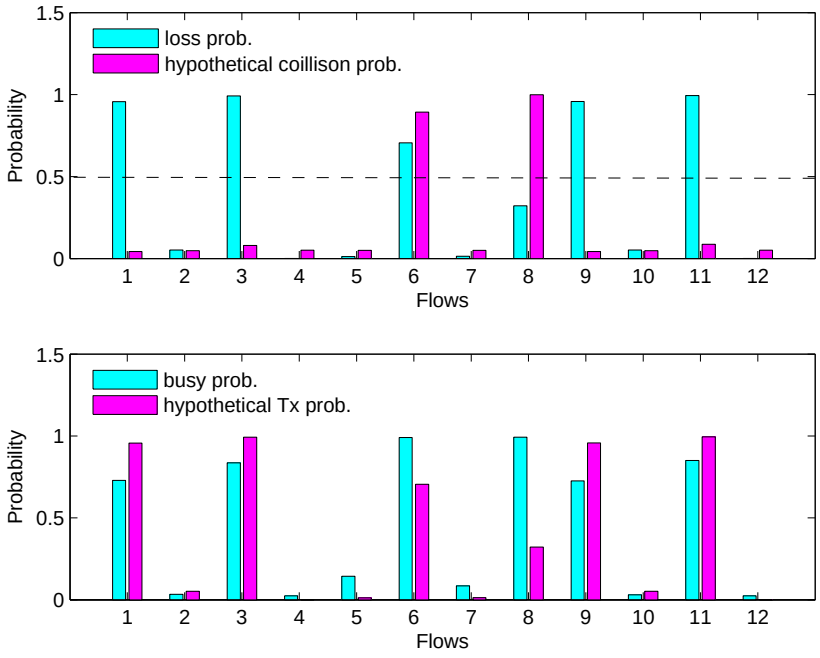

Fig. 10: Flow packet loss and hypothetical collision probability in grid network

From Fig. 11, we see that most flows suffering from hidden node starvation concentrate at the upper left corner, flows with carrier sensing starvation stay at the lower section whereas flows contending with many coordinate flows are in the middle. By setting $\alpha = 1.5$, one can distinguish with high probability three cases. To study the effect of α, we list in Table II the correct and miss identification probabilities by categories. We can see that the best value of α is around 1.5 – 2.0, where high correct identification and low miss classification can be achieved.

TABLE II: Setting of parameter α("C"– coordinated nodes, "S"–carrier sense starvation, "H"– hidden node starvation)

α	Correct Prob.			Miss Prob.					
	C	S	H	C-S	C-H	S-C	S-H	H-C	C-S
1.0	0.00	0.99	0.98	0.22	0.78	0.00	0.01	0.00	0.02
1.5	0.74	0.96	0.98	0.03	0.24	0.02	0.01	0.01	0.01
2.0	0.95	0.88	0.97	0.01	0.04	0.11	0.01	0.02	0.01
2.5	0.96	0.78	0.95	0.00	0.04	0.21	0.01	0.05	0.00

Fig. 12 plots the busy probability and x^H of flows that are classified as hidden node starvation in Fig. 11. We further classify them as asymmetric sense starvation and regular hidden node starvation by setting $\beta = 1$. As expected, the busy probabilities of links with only hidden node starvation are normally lower than the hypothetical Tx probabilities, while the links experiencing asymmetric sense starvation have higher busy probabilities. The effect of β is summarized in Table III. We can see the the best value of β is around 0.8 – 1.0.

TABLE III: Setting of parameter β ("H"–hidden node starvation, "A"–asymmetric sense starvation, "H/A"– both)

β	Correct Prob.		Miss Prob.			
	H	A	H-H/A	H-A	A-H/A	A-H
0.8	1.00	0.87	0.00	0.00	0.00	0.13
1.0	0.96	0.60	0.00	0.04	0.00	0.40
1.5	0.89	0.28	0.11	0.00	0.64	0.08

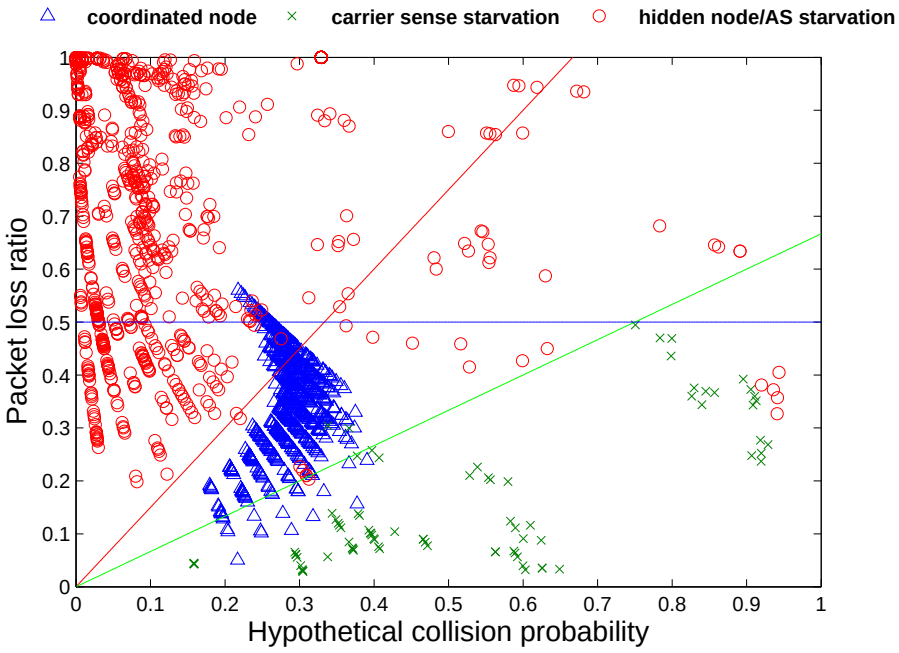

Fig. 11: Loss probability vs. collision probability of starved flows in 50 randomly generated networks. Diagonal straight lines correspond to $\alpha = 1.5$, the horizontal line for $p = 0.5$

VII. Conclusions

In this paper, we have developed models to analyze the individual throughput of nodes in high density 802.11 wireless community networks. We have shown that our model can correctly predict the flow throughput and analyze the root causes of the starvation problem. Based on the insight from theoretical analysis and simulation results, we design a simple identification mitigation algorithm that utilizes local measurement and theoretical inference. Simulation results demonstrate the effectiveness of the proposed algorithm.

References

[1] The network simulator - ns2. http://www.isi.edu/nsnam/ns/.
[2] A. Akella, G. Judd, S. Seshan, and P. Steenkiste. Self-management in chaotic wireless deployments. In *MobiCom'05*, 2005.
[3] Y. Bejerano, S.-J. Han, and L. E. Li. Fairness and load balancing in wireless LANs using association control. In *Mobicom'04*, 2004.
[4] G. Bianchi. Performance analysis of the IEEE 802.11 distributed coordination function. *IEEE JSAC*, 18(3):535–547, 2000.
[5] F. Cali, M. Conti, and E. Gregori. Dynamic tuning of the IEEE 802.11 protocol to achieve a theoretical throughput limit. *IEEE/ACM Trans. on Networking*, 8(6):785–799, 2000.
[6] Y.-C. Cheng, J. Bellardo, P. Benko, A. C. Snoeren, G. M. Voelker, and S. Savage. Jigsaw: solving the puzzle of enterprise 802.11 analysis. In *SIGCOMM'06*, 2006.
[7] Y. Gao, D. Chiu, and J. Lui. Determining the end-to-end throughput capacity in multi-hop networks: Methodology and applications. In *ACM Sigmetrics/Performance 2006*, 2006.
[8] M. Garetto, T. Salonidis, and E. Knightly. Modeling per-flow throughput and capturing starvation in csma multi-hop wireless networks. In *IEEE INFOCOM'06*, 2006.
[9] R. Jain, D. Chiu, and W. Hawe. A quantitative measure of fairness and discrimination for resource allocation in shared systems. DEC Research Report TR-301, 1985.
[10] J. Kim, S. Kim, S. Choi, and D. Qiao. CARA: Collision-aware rate adaptation for IEEE 802.11 wlans. In *IEEE INFOCOM'06*, 2006.
[11] T.-S. Kim, J. C. Hou, and H. Lim. Improving spatial reuse through tuning transmit power, carrier sense threshold, and data rate in multihop wireless networks. In *MobiCom'06*, pages 366–377, Los Angeles, CA, USA, 2006. ACM Press.
[12] T.-Y. Lin and J. C. Hou. Interplay of spatial reuse and sinr-determined data rates in csma/ca-based, multi-hop, multi-rate wireless networks. In *Infocom'07*, 2007.
[13] R. Mahajan, M. Rodrig, D. Wetherall, and J. Zahorjan. Analyzing the mac-level behavior of wireless networks in the wild. In *SIGCOMM'06*, 2006.
[14] V. Mhatre, K. Papagiannaki, and F. Baccelli. Interference mitigation through power control in high density 802.11 WLANs. In *Infocom'07*, 2007.
[15] A. Mishra, V. Brik, S. Banerjee, A. Srinivasan, and W. Arbaugh. A client-driven approach for channel management in wireless lans. In *IEEE Infocom'06*, 2006.

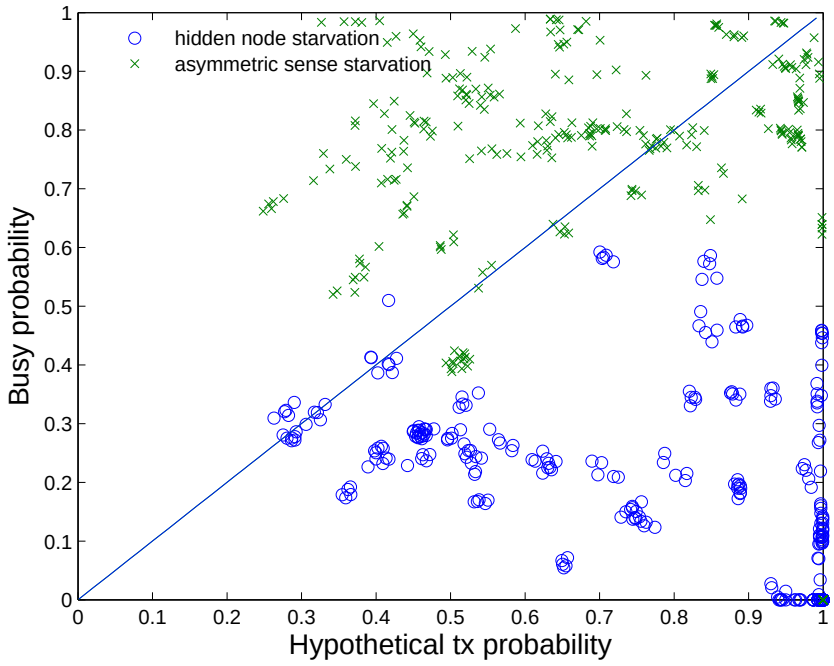

Fig. 12: Identification of hidden node and asymmetric sense starvation. The straight line corresponds to $\beta = 1$

[16] A. Mishra, E. Rozner, S. Banerjee, and W. Arbaugh. Exploiting partially overlapping channels in wireless networks: Turning a peril into an advantage. In *IMC'05*, 2005.

[17] A. Mishra, S. Shrivastava, V. Banerjee, and W. Arbaugh. Partially overlapped channels not considered harmful. In *ACM Sigmetrics'06*, 2006.

[18] A. Mishra, V. Shrivastava, D. Agrawal, S. Banerjee, and S. Ganguly. Distributed channel management in uncoordinated wireless environments. In *Mobicom*, 2006.

[19] J. Shi, T. Salonidis, and E. Knightly. Starvation mitigation through multi-channel coordination in csma based wireless networks. In *ACM MobiHoc 2006*, 2006.

[20] A. Vasan, R. Ramjee, and T. Woo. Echos - enhanced capacity 802.11 hotspots. In *IEEE Infocom'05*, 2005.

[21] K. Wang, F. Yang, Q. Zhang, and Y. Xu. Modeling path capacity in multi-hop ieee 802.11 networks for qos services. *IEEE Transactions on Wireless Communications*, 6(2):738–749, 2007.

[22] S. H. Y. Wong, S. Lu, H. Yang, and V. Bharghavan. Robust rate adaptation for 802.11 wireless networks. In *Proceedings of the 12th annual international conference on Mobile computing and networking*, pages 146–157, Los Angeles, CA, USA, 2006. ACM Press.

[23] X. Yang and N. Vaidya. On physical carrier sensing in wireless ad hoc networks. In *INFOCOM 2005.*, volume 4, pages 2525–2535 vol. 4, 2005.

[24] H. Zhai and Y. Fang. Physical carrier sensing and spatial reuse in multirate and multihop wireless ad hoc networks. In *INFOCOM 2006.*, 2006.